Phys. Status Solidi A **211,** No. 11, 2558–2562 (2014) / **DOI** 10.1002/pssa.201431315

physica status solidi a
www.pss-a.com
applications and materials science

Forward current enhanced elimination of the radiation induced boron–oxygen complex in silicon n^+–p diodes

L. F. Makarenko[*,1], S. B. Lastovskii[,2], H. S. Yakushevich[2], M. Moll[3], and I. Pintilie[4]**

[1] Belarusian State University, Independence Ave. 4, 220030 Minsk, Belarus
[2] Scientific-Practical Materials Research Centre of NAS of Belarus, P. Brovka Str. 19, 220072 Minsk, Belarus
[3] CERN, 1211 Geneva 23, Switzerland
[4] National Institute of Materials Physics, Str. Atomistilor 105bis, Magurele, Romania

Received 25 April 2014, revised 18 June 2014, accepted 18 June 2014
Published online 22 July 2014

Keywords defect complexes, diodes, radiation-induced defects, silicon, solar cells

[*] Corresponding author: e-mail makarenko@bsu.by, Phone: +375 17 209 5075, Fax: +375 17 209 5104
[**] e-mail lastov@ifttp.bas-net.by, Phone: +375 17 284 4289, Fax: +375 17 284 1558

Using forward current injection with densities in the range 15–30 A/cm^2 we can effectively eliminate the radiation-induced boron–oxygen complex, which is the main compensating center in irradiated Si solar cells. It was found that for a given forward current density the elimination rate is decreasing with increasing irradiation dose. Additionally, some evidences have been obtained on the negative-*U* properties of the radiation-induced boron–oxygen complex.

1 Introduction Recombination enhancement of defect reactions is typically observed in compound semiconductors [1, 2]. In silicon, the recombination enhancement of migration was found to be characteristic for many single interstitial atoms formed as result of irradiation. These are silicon self-interstitial (Si_i) [3], aluminum interstitial (Al_i) [4], boron interstitial (B_i) [5] and carbon interstitial (C_i) [6].

The enhancement of defect reactions often helps to recover the original properties of the devices that were deteriorated by irradiation. It has been shown previously that the recombination enhanced annealing occurring under minority carrier injection increases the radiation tolerance of InP solar cells above that of Si based devices [7]. One of the mechanisms for Si solar cells degradation under irradiation is compensation of the initial charge carrier concentration [8]. It has been shown that the main compensating center in boron-doped Si solar cells is the radiation-induced boron–oxygen center [8]. This center was found to have a donor level at $E_c-0.23$ eV [5] and was identified as interstitial boron–interstitial oxygen complex (B_iO_i) [9]. It is stable at room temperature and begins to anneal at 150 °C. Activation energy of its thermal annealing in irradiated samples was determined in Refs. [8, 10] to be $E_a = 1.2$ eV. However, more recent studies [11, 12] reported slightly higher values $E_a = 1.35$–1.4 eV. The annealing rate increases with the increase of the boron concentration [11] and the decrease of oxygen content [12].

Another process where boron–oxygen interaction plays an important role is the light-induced degradation of Si solar cells. This process is characterized by much lower activation energies, one initial fast process with an activation energy around 0.2 eV followed by a slow degradation process with activation energies between 0.4 and 0.5 eV [13]. It was suggested that the degradation is associated with the formation of boron–oxygen dimer centers (B_iO_{2i} or B_sO_{2i}) [14–16]. According to the model proposed in Ref. [15] the formation of B_iO_{2i} complex can explain these degradation features. However, recent theoretical calculations [16] showed that the formation energy of B_i is very high and its concentration is negligible. The present letter reports on the forward current enhanced (FCE) annealing of B_iO_i defect complex at ambient or lower temperatures, showing that upon minority carrier injection the necessary energy for releasing the B_i from B_iO_i complex can be essentially reduced by electronic subsystem excitation.

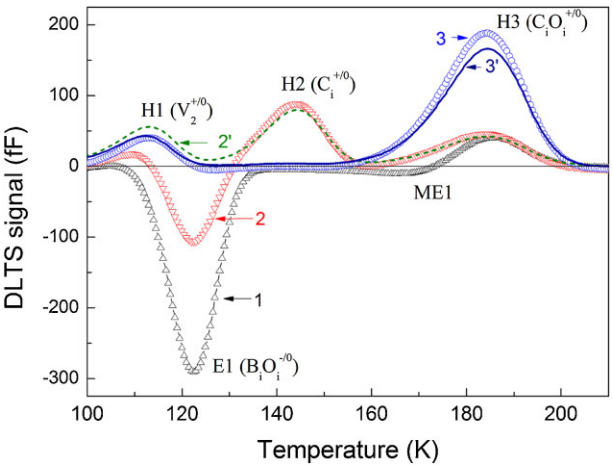

Figure 1 MC-DLTS (open symbols, curves 1, 2, and 3) and conventional DLTS (line curves 2′ and 3′) spectra obtained on samples irradiated for 100 min. The curve 1 represents MC-DLTS spectra obtained after irradiation and preliminary annealing for 30 min at 120 °C. The curves 2 and 2′ were recorded after 20 min of FCE annealing at 280 K and the curves 3 and 3′ after the complete elimination of B_iO_i (E1) and transformation of C_i (H2) into C_iO_i (H3).

2 Experimental Epitaxial Si n^+–p structures (diodes) have been used in our experiments. The hole concentration in these structures was estimated from capacitance–voltage measurements to be $(0.8 \pm 0.1)\,10^{15}\,cm^{-3}$ and is mainly due to the doping with boron during the epitaxial growth of the used silicon. The oxygen content in all of the structures is about $[O] = 1.5 \times 10^{17}\,cm^{-3}$ as determined by the annealing rate of interstitial carbon using the calibration presented in [17]. The carbon concentration in epitaxial silicon is usually much less than typical values for Czochralski-grown crystals (see for example, SIMS results in Ref. [18]) and has a value close to the concentration of boron in our samples. This fact is supported further by the ratio between the amplitudes of DLTS peaks related to boron and carbon defects shown in Fig. 1. Irradiations with α-particles from a Pu-239 surface source were performed at about 280–290 K. Its surface activity was about $2 \times 10^8\,Bq/cm^2$. The alpha-particle energies were 5.144 and 5.157 MeV and the irradiation time was 1–15 h. The damage distribution of the irradiation source was described in Ref. [17].

The electrically active defects induced by irradiation with α-particles were investigated by means of the Deep Level Transient Spectroscopy (DLTS) technique applied in a temperature range of 79–270 K. Further on we will use two notations for the recorded spectra: DLTS, when injection pulses are performed with majority-carriers (0 V or reverse bias filling pulses) and MC-DLTS when also minority carriers are injected during the pulses (forward bias filling pulses).

3 Formation of the defects Production of isolated vacancies and self-interstitial during irradiation of a silicon crystal initiates a series of defect reactions, which is expected to end only when defect complexes that are stable at the irradiation temperature are formed. In boron-doped silicon irradiated with α-particles the formation of defects stable at room temperature requires a rather long time, which often exceeds the irradiation time. This is mainly due to the relatively low mobility of Si self-interstitials [19]. At the end of the defect reaction series, two main radiation induced complexes of interstitial type are formed in boron-doped silicon. These are interstitial carbon interstitial–oxygen interstitial (C_iO_i) and interstitial boron–interstitial oxygen (B_iO_i) complexes.

To complete the formation of interstitial defects at room temperatures one needs to wait long time (more than a week) [19]. To accelerate these defect reactions we performed a preliminary thermal annealing of the irradiated samples at 120 °C for 30 min. The obtained MC-DLTS spectrum after annealing is the curve 1 in Fig. 1. Two main majority carrier peaks (H1 and H3) and one minority carrier peak (E1) are recorded and they are related to the well-known defects: divacancy (H1), C_iO_i (H3), and B_iO_i (E1), respectively [9, 10]. It was found earlier [9] that the substitutional boron has 7 times larger capture radius for Si self-interstitials than the carbon interstitial. Thus, the large amplitude of the E1 peak as compared with that of the H3 peak means that the carbon concentration in our structures is much lower than $10^{16}\,cm^{-3}$. Another irradiation induced electron trap (ME1 in Fig. 1) of unknown nature is observed. It displays a metastable behavior that is revealed when using cycling of thermal annealing and forward current injection. This trap is not observed immediately after irradiation but appears after annealing at 120 °C.

4 Annealing studies All these complexes, observed after the preliminary annealing for 30 min at 120 °C, are stable at room temperature. Under thermal equilibrium they anneal-out at different temperatures: B_iO_i at 150–200 °C, V_2 at 250–300 °C, and C_iO_i at 375–425 °C [9]. However, we have found that the B_iO_i complex can be eliminated already at room temperature by a forward current injection. Forward current densities of 10–30 A/cm^2 are required to have a fairly high rate (with characteristic time constant of about several minutes) of this process at room temperature. When the FCE annealing temperatures are relatively low (lower than 290 K) the loss of the E1 peak amplitude is accompanied by the growth of the H2 peak only (compare curve 1 with curve 2 in Fig. 1). From its DLTS signature we identified the latter one as the interstitial carbon. This defect is known to be mobile at room temperature and can be trapped by interstitial oxygen. This reaction is also observed in our structures as the loss of the H2 peak (C_i) has a one-to-one relation to the growth of the H3 peak (C_iO_i) (not shown here). At higher FCE annealing temperatures we observe either the growth of both H2 (C_i) and H3 (C_iO_i) peaks (below 50 °C) or the growth of the H3 peak only (above 50 °C). At the end of both, the complete FCE annealing of B_iO_i and the trapping of all mobile carbon interstitials by oxygen, we detect only the divacancy (H2) and the C_iO_i (H3) peaks (curves 3 and 3′ in

Fig. 1). Following the increase of the H2 + H3 peak amplitudes after different durations of the FCE annealing and comparing them with the decrease in amplitude of the E1 peak, a linear correlation is found for three different FCE temperatures. This is depicted in Fig. 2.

These results demonstrate that the annealing of the B_iO_i complex (E1 peak) is accompanied by the appearance of interstitial carbon (H2 peak). In our opinion, such a process can occur considering three consecutive defect reactions: (i) the recombination enhanced dissociation of B_iO_i and appearance of B_i, (ii) an inverse Watkins replacement reaction for interstitial boron

$$B_i + Si_s + M \rightarrow B_s + Si_i + M^*, \quad (1)$$

and (iii) a direct Watkins replacement reaction for substitutional carbon

$$C_s + Si_i \rightarrow C_i. \quad (2)$$

As M in reaction (1) we denote a possible mediator or a component of an intermediate complex.

As seen from Fig. 2 the correlation between the decrease in the E1 peak height and the increase in the sum of the H2 and H3 peak heights can be expressed by the following equation:

$$\frac{1}{2}\delta S_{E1} + \delta S_{H2} + \delta S_{H3} = 0, \quad (3)$$

where δS_{E1}, δS_{H2}, and δS_{H3} are the changes of the absolute values of heights for the E1, H2, and H3 peaks, respectively. Equation (3) evidences that the height of the E1 peak (B_iO_i) is determined by the emission of two electrons. This property is characteristic for negative-U defects [5]. Thus, one can presume that the B_iO_i complex inherits the negative-U properties of the interstitial boron [5]. It means, primarily, that the energy level E_c −0.23 eV, which corresponds to the E1 trap is an acceptor level of B_iO_i and, secondly, that this complex has a shallower donor level $E(0/+)$.

The B_iO_i concentration decreases exponentially with annealing time (see Fig. 3). The rate of the FCE annealing depends on the forward current density (compare curves 1 and 2 in Fig. 3), annealing temperature and irradiation dose (compare curves 1 and 1′ in Fig. 3). Experiments at different temperatures showed that the FCE annealing rate changes approximately quadratically with the injection current density, similar to the FCE annealing of the interstitial boron [5]. As seen from Fig. 3 the lower the irradiation dose is the higher is the annealing rate for the same forward current density and temperature. This fact can be explained as a result of the decrease of minority carrier lifetime with irradiation dose [20, 21].

We have performed isochronal annealing studies of B_iO_i and C_iO_i complexes, up to 400 K for the FCE annealing and up to 700 K for thermal annealing. The obtained defect concentrations (N) normalized to the defect initial density (N_0, measured after the preliminary annealing at 120 °C) are given in Fig. 4.

Some of the obtained results (curves 1 and 1′ in Fig. 4) are consistent with previous results on the thermal stability of B_iO_i and C_iO_i complexes [9]. They also show that an essential growth of C_iO_i defect concentration takes place at 300–350 °C. Such an increase of C_iO_i concentration during annealing at $T_{ann} \geq 300$ °C was observed in many works, see for example, the results of IR spectroscopy studies presented in Ref. [22]. However, in our structures the C_iO_i increase is rather large compared to the one observed in Czochralski-grown crystals [22]. We consider that this difference is due to the relatively low carbon content in our structures that are based on epitaxial silicon. In Czochralski-grown materials most of the Si self-interstitial formed under bombardment are

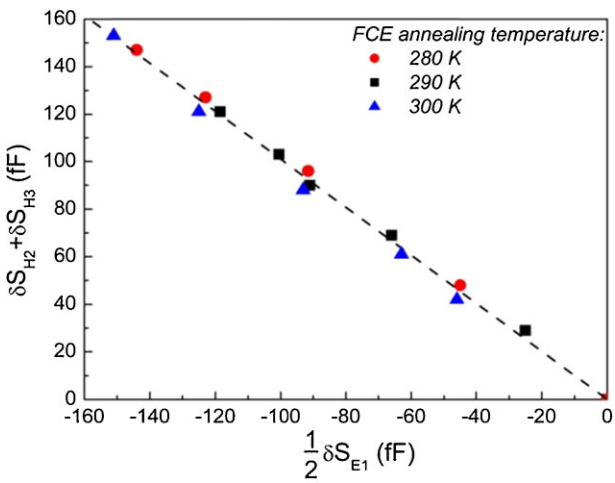

Figure 2 Correlation between the increase of the (H2 + H3) DLTS peak heights and the decrease of the E1 MC-DLTS peak height during the FCE annealing at different temperatures. The line shows the least squares fitting of experimental data (points).

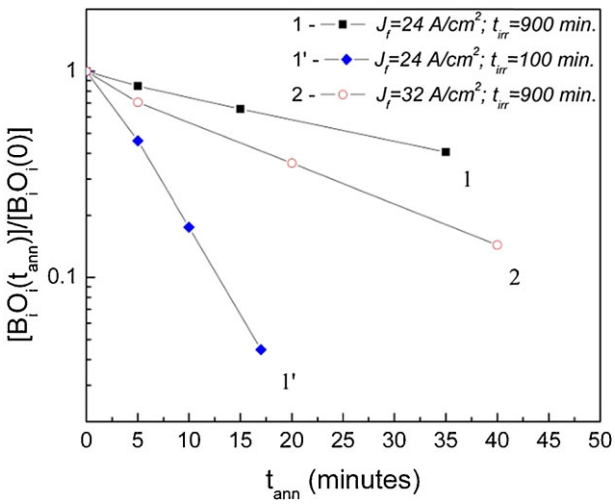

Figure 3 Kinetics of B_iO_i disappearance during the isothermal FCE annealing at 300 K (t_{ann}) for different forward current densities (J_f) and for different irradiation times (t_{irr}).

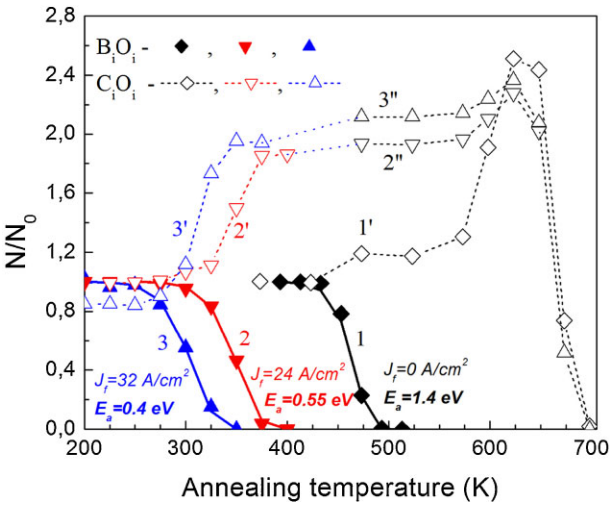

Figure 4 Isochronal annealing behavior of B_iO_i (filled symbols) and C_iO_i (empty symbols) complexes, in steps of 25 K, for samples irradiated for 900 min. Results of the 30 min thermal annealing ($J_f = 0$ A/cm^2) at each temperature are given by the curves 1, 1′, and 2″, 3″. The FCE annealing was performed between 200 K and 400 K for 10 min at each temperature and for two different forward currents: $J_f = 24$ A/cm^2 (curves 2, 2′) and $J_f = 32$ A/cm^2 (curves 3, 3′). The fitting curves for the B_iO_i annealing are given as thick solid lines.

trapped by substitutional carbon (C_s) immediately after irradiation. In our crystals with relatively low carbon content only a part of the radiation-formed Si_i is trapped by C_s and only after the annealing of other interstitial complexes an additional growth of C_iO_i can be observed.

According to the thermal annealing data presented in Fig. 4 (curves 1 and 1′), no direct correlation between the growth of C_iO_i and the annealing-out of B_iO_i exists. While the B_iO_i anneals-out completely at 200 °C the increase in the concentration of C_iO_i is observed only above 300 °C. Under FCE annealing, however, the increase in C_iO_i concentration takes place already at room temperature and simultaneously with the decrease in the B_iO_i density (curves 2, 2′ and 3, 3′ in Fig. 4). Furthermore, the FCE-induced generation of C_iO_i leads to defect concentrations that are very close to those obtained after thermal annealing (in absence of FCE) at temperatures above 300 °C (compare curve 1′ with curves 2″ and 3″ in Fig. 4). Also, after the FCE annealing a subsequent thermal annealing at $T \geq 300$ °C produces only a relatively small increase of the H3 (C_iO_i) peak height (see curves 2″ and 3″ in Fig. 4). It means that the two reactions, dissociation of B_iO_i and formation of C_iO_i, taking place during the thermal annealing at different temperatures, are both enhanced by the forward current injection, resulting in much lower activation energies for the FCE annealing than those corresponding to the thermal annealing. All these energies can be evaluated by fitting the isochronal annealing data.

The fitting results for the FCE annealing of B_iO_i complex are shown by lines 1–3 in Fig. 4. The resulting activation energies are in the range of $E_a = 0.4$–0.6 eV for current densities between 15 and 30 A/cm^2 and are close to those reported for the slowly forming recombination center in illuminated p-type silicon. The activation energy increases when lowering the injection current densities. This observation is consistent with earlier results reported for Si and GaAs [4, 5, 23]. For zero current density, the activation energy for the annealing of B_iO_i was reported previously to be of about 1 eV larger, i.e., $E_a \sim 1.4$ eV (curve 1 in Fig. 4) consistent with the results of Refs. [11, 12]. Thus, the presently reported FCE annealing procedure leads to a significant decrease in the activation energy for the annealing of the B_iO_i complex ($\Delta E_a \sim 1$ eV), similar to the case of interstitial aluminum and boron in silicon [4, 5].

5 Summary Using forward current injection at room temperature we can eliminate the radiation-induced boron–oxygen complex, which is the main compensating center in irradiated Si solar cells. To achieve a high enough elimination rate, relatively high current densities are required. Besides, new evidences have been obtained on the relation between interstitial carbon–oxygen complex growth at 350–400 °C and interstitial boron–oxygen complex annealing in Si crystals.

Acknowledgements This work has been carried out in the framework of the RD50 CERN Collaboration. Partial financial support from the BRFFR (Belarus) and Romanian Academy of Sciences under the Grant No. F12RA-005 as well from the Romanian Authority for Scientific Research through the Project PCE 72/5.10.2011 is gratefully acknowledged.

References

[1] L. C. Kimerling, Solid-State Electron. **21**, 1391 (1978).
[2] D. V. Lang, Ann. Rev. Mater. Sci. **12**(1), 377 (1982).
[3] G. D. Watkins, Radiation Damage in Semiconductors (Dunod, Paris, 1965), p. 97.
[4] J. R. Troxell, A. P. Chatterjee, G. D. Watkins, and L. C. Kimerling, Phys. Rev. B **19**, 5336 (1979).
[5] J. R. Troxell and G. D. Watkins, Phys. Rev. B. **22**, 921 (1980).
[6] A. R. Frederickson, A. S. Karakashian, P. J. Drevinsky, and C. E. Caefer, J. Appl. Phys. **65**, 3272 (1989).
[7] M. Yamaguchi, K. Ando, A. Yamamoto, and C. Uemura, Appl. Phys. Lett. **44**, 432 (1984).
[8] A. Khan, M. Yamaguchi, Y. Ohshita, N. Dharmarasu, K. Araki, T. Abe, H. Itoh, T. Oshima, M. Imaizimi, and S. Matsuda, J. Appl. Phys. **90**, 1170 (2001).
[9] L. C. Kimerling, P. J. Drevinsky, J. L. Benton, M. T. Asom, and C. E. Caefer, Mater. Sci. Forum **38**, 141 (1991).
[10] P. M. Mooney, L. J. Cheng, M. Süli, J. D. Gerson, and J. W. Corbett, Phys. Rev. B **15**, 3836 (1977).
[11] O. V. Feklisova, N. A. Yarykin, and J. Weber, Semiconductors **47**, 228 (2013).
[12] L. F. Makarenko, S. B. Lastovskii, F. P. Korshunov, M. Moll, I. Pintilie, and N. V. Abrosimov, AIP Conf. Proc. **1583**, 123 (2014).
[13] H. Hashigami, M. Dhamrin, and T. Saitoh, Jpn. J. Appl. Phys. **42**, 2564 (2003).

[14] L. I. Murin, E. A. Tolkacheva, V. P. Markevich, A. R. Peaker, B. Hamilton, E. Monakhov, B. G. Svensson, J. L. Lindstrom, P. Santos, J. Coutinho, and A. Carvalho, Appl. Phys. Lett. **98**, 182101 (2011).
[15] V. V. Voronkov and R. Falster, J. Appl. Phys. **107**, 053509 (2010).
[16] A. Carvalho, P. Santos, J. Coutinho, R. Jones, M. J. Rayson, and P. R. Briddon, Phys. Status Solidi A **209**, 1894 (2012).
[17] L. F. Makarenko, M. Moll, F. P. Korshunov, and S. B. Lastovski, J. Appl. Phys. **101**, 113537 (2007).
[18] I. Pintilie, G. Lindstroem, A. Junkes, and E. Fretwurst, Nucl. Instrum. Methods Phys. Res. A **611**, 52 (2009).
[19] L. F. Makarenko, M. Moll, J. H. Evans-Freeman, S. B. Lastovski, L. I. Murin, and F. P. Korshunov, Physica B **407**, 3016 (2012).
[20] S. D. Brotherton and P. Bradley, J. Appl. Phys. **53**, 5720 (1982).
[21] A. Hallen, N. Keskitalo, F. Masszi, and V. Nágl, J. Appl. Phys. **79**, 3906 (1996).
[22] L. I. Murin, V. P. Markevich, J. L. Lindström, M. Kleverman, J. Hermansson, T. Hallberg, and B. G. Svensson, Solid State Phenom. **82**, 57 (2001).
[23] D. Stievenard, X. Boddaert, J. C. Bourgoin, and H. J. Von Bardeleben, Phys. Rev. B **41**, 5271 (1990).

